Sound Transmission Properties of Mineral-filled High-Density Polyethylene (HDPE) and Wood-HDPE Composites

Birm-June Kim,[a,b] Runzhou Huang,[c] Xinwu Xu,[c] Sun-Young Lee,[d,*] Jason Kunio,[e] and Qinglin Wu [b,c*]

Wood plastic composites (WPCs) offer various advantages and potential as a competitive alternative to conventional noise barriers. For this purpose, the influence of composite formulation on the sound transmission loss (*TL*) of WPCs needs to be fully understood. In *TL* testing, stiffness and surface density are major factors influencing the sound insulation property of filled plastics and WPCs. Experimental *TL* values decreased as sound frequency increased; and the TL values increased after passing a certain frequency level. The comparison of experimental *TL* curves among filled composites showed that the addition of fillers led to an increase in resonance frequency and *TL* values. However, at high filling levels, the stiffness decrease led to *TL* reductions. The experimental *TL* curves of filled composites, composed of mass law and stiffness law predictions, were well approximated with their combined *TL* predictions.

Keywords: Clay; Calcium carbonate; Wood plastic composites; Sound transmission loss

*Contact information: a: Department of Forest Products and Biotechnology, Kookmin University, Seoul 136-702, Korea; b: School of Renewable Natural Resources, Louisiana State University AgCenter, Baton Rouge, Louisiana 70803, USA; c: College of Material Science and Engineering, Nanjing Forestry University, Nanjing, 210037, China; d: Korea Forest Research Institute, Seoul 130-712, Korea; e: Brüel & Kjær North America, USA; *Corresponding authors: qwusfm@gmail.com and nararawood@forest.go.kr*

INTRODUCTION

Industrial machinery and high speed transportation produces unwanted noise (Jayaraman 2005; Yilmaz 2009). For example, highway noise levels amount to 70 dB, and noise levels from highly-trafficked urban road intersections amount up to 80 dB (Kotzen and English 1999). Excessive noises frequently affect people and can cause fatigue, health system disorders, and can reduce working efficiency. So far, various barrier materials including concrete, brick, metal, plastic, wood, and composites have been used to reduce noise levels. Among these materials, viscoelastic polymer materials show great potential for damping sound and vibration. However, most polymer materials have a relatively low elastic modulus and surface density, leading to poor sound insulating performances when used alone as noise barriers (Wang *et al.* 2011).

Significant work has recently investigated the acoustic properties of filled plastic composites. Among the studies, Lee *et al.* (2010) investigated tensile and sound transmission loss (*TL*) properties of composites made of acrylonitrile butadiene styrene (ABS) and carbon-black. In their experiments, it was shown that composites filled with 5% carbon-black had a more than 10% *TL* increase compared with the unfilled control. The composites with a high elastic modulus showed a higher *TL* than the composites with a low elastic modulus. As a result, it was suggested that an increase in modulus through

reinforcing the composite structure could be an effective technique for blocking sound energies. Lee *et al.* (2008) studied the sound insulation effect of carbon-nanotube (CNT) filled ABS composites. As CNT content in the ABS composites increased, *TL* values were accordingly improved. For example, at 3400 Hz, the average *TL* value of CNT filled composites with 15% volume content was 21.7% higher than that of ABS-only composite. Also, it was shown that increased stiffness due to higher CNT content had a more significant effect on the *TL* value of CNT-filled composites than an increase in mass. Cotana *et al.* (2007) evaluated *TL* properties of concrete composites filled with different densities of pumice, lapillus, and rubber. Various combinations of composite compositions made a noticeable influence on the *TL* properties. The *TL* values of lapillus/pumice mixture filled composites were higher than those of lapillus-only and pumice-only filled composites. Among the mixtures, the lapillus/pumice filled composite showed a higher *TL* value compared with the pumice/rubber filled composite. This was due to the overall change in density of the composites made with fillers of varying densities. Wang *et al.* (2011) studied the *TL* of laminated mica-filled poly (vinyl chloride) composites which showed increased *TL* and resonance frequency with the increase of mica content. In the current study, stiffness and surface density were found to be important factors influencing the *TL* properties of mica filled composites. The sound insulation properties of the composites were well described by stiffness and mass laws.

Wood plastic composites (WPCs) as new generation green composites offer the advantages of having relatively light weight, excellent recyclability, low toxicity, and high thermal stability (Klyosov 2007; Wu *et al.* 2007; Kim *et al.* 2012). WPCs are currently used as deck, fence, outdoor furniture, and interior molding materials. Thus, their application as a noise barrier can offer competitive alternatives to conventional noise barriers. For this purpose, the influence of composite formulations on the acoustic properties of WPCs needs to be fully understood.

The objectives of this study were 1) to develop an experimental procedure for studying the *TL* properties of filled plastic composites using an impedance tube method, and 2) to investigate the effect of mineral type and loading levels on the observed *TL* properties of the composites in comparison with various *TL* predictions.

Impedance Tube

The impedance tube system, based on the ASTM E2611-09 standard (ASTM E2611, 2009) for measuring the normal incidence transmission loss (*TL*) is schematically illustrated in Fig 1a. The *TL* results is calculated with two microphones positioned at the upstream and two more microphones positioned downstream of the test sample as shown in Fig. 1b. In this system, sound pressures at the four measurement locations x1 to x4 can be expressed as super-positions of positive and negative directed plane waves (±jkx) (Song and Bolton 2000; Olivieri *et al.* 2007),

$$\begin{cases} P_1 = Ae^{-jkx_1} + Be^{jkx_1} \\ P_2 = Ae^{-jkx_2} + Be^{jkx_2} \\ P_3 = Ce^{-jkx_3} + De^{jkx_3} \\ P_4 = Ce^{-jkx_4} + De^{jkx_4} \end{cases} \quad (1)$$

where, k is the wave number in ambient air, and parameters A to D are complex plane wave coefficients representing the noise amplitudes. This equation can be rearranged to solve for the respective coefficients in terms of the four sound pressures (P_1 to P_4) as:

$$\begin{cases} A = \dfrac{j(P_1 e^{jkx_2} - P_2 e^{jkx_1})}{2\sin k(x_1 - x_2)} \\ B = \dfrac{j(P_2 e^{-jkx_1} - P_1 e^{-jkx_2})}{2\sin k(x_1 - x_2)} \\ C = \dfrac{j(P_3 e^{jkx_4} - P_4 e^{jkx_3})}{2\sin k(x_3 - x_4)} \\ D = \dfrac{j(P_4 e^{-jkx_3} - P_3 e^{-jkx_4})}{2\sin k(x_3 - x_4)} \end{cases} \quad (2)$$

Therefore, by measuring the sound pressures at locations x_1 to x_4, the coefficients A to D are determined, and these coefficients provide the input data for subsequent transfer matrix calculations (Song and Bolton 2000; Olivieri *et al.* 2007; Yousefzadeh *et al.* 2008). The transfer matrix, relating with sound pressures (P) and particle velocities (V) at the two surfaces (front and rear) of the test sample extending from x=*0* (front) to x=*d* (rear) has the following form (Olivieri *et al.* 2006, 2007),

$$\begin{bmatrix} P \\ V \end{bmatrix}_{x=0} = \begin{bmatrix} T_{11} & T_{12} \\ T_{21} & T_{22} \end{bmatrix} \begin{bmatrix} P \\ V \end{bmatrix}_{x=d} \quad (3)$$

where, T_{ij} are frequency-dependent quantities related to the acoustical properties of the test sample. Thus, the P and V at the two surfaces of the test sample can be effectively expressed by the positive and negative plane wave components $\pm jkx$ and complex coefficients,

$$P\big|_{x=0} = A + B \quad (4a)$$

$$V\big|_{x=0} = \frac{A - B}{\rho_0 c} \quad (4b)$$

$$P\big|_{x=d} = Ce^{-jkd} + De^{jkd} \quad (4c)$$

$$V\big|_{x=d} = \frac{Ce^{-jkd} - De^{jkd}}{\rho_0 c} \quad (4d)$$

where ρ_0 is ambient air density and c is the sound speed in air. When the plane wave components are known, based on the measurements of complex pressures at the four locations, the P and V values at the two surfaces of the test sample can be determined.

The 2x2 transfer matrix described in Eq. 3 cannot be solved without some additional information, as there are four unknowns but a single measurement only results in two equations. If the test sample is geometrically symmetric (presenting the same physical properties to the sound field on either side), then some basic constraint equations

can be applied due to reciprocity, namely $T_{11} = T_{22}$ and $T_{11}T_{22} - T_{12}T_{21} = 1$. In practice it is more common to use the two load method to generate two additional equations needed to solve the 2x2 transfer matrix. This is done by changing the end condition of the measurement tube. This effectively changes the impedance at the termination, hence making it possible to rewrite Eq. 3 as follows:

$$\begin{bmatrix} P^{(a)} & P^{(b)} \\ V^{(a)} & V^{(b)} \end{bmatrix}_{x=0} = \begin{bmatrix} T_{11} & T_{12} \\ T_{21} & T_{22} \end{bmatrix} \begin{bmatrix} P^{(a)} & P^{(b)} \\ V^{(a)} & V^{(b)} \end{bmatrix}_{x=d} \quad (5)$$

Generally, the two loads can be represented by two different length tubes or a single tube with and without absorbing material. In this research, two loads were achieved by a tube with and without absorbing material.

In addition to the normal incidence transmission loss (TL_{normal}) term, there are many other acoustic properties of the material that can be calculated from the elements in the transfer matrix, as described in the ASTM E2611-09 standard. These other characteristics can be used to generate macroscopic models of the material for further material development to optimize a materials performance based on the Biot model (Raveendra *et al.* 2005). Work has also been done to use these measured normal incidence results to predict materials performance in a random incidence environment (Yoo *et al.* 2005).

Consequently, when a two-load method with a perfectly anechoic termination (*i.e.*, *D=0*) is used, *TL* is calculated as:

$$TL_{normal}(dB) = 10\log_{10}\left(\frac{1}{4}\left|T_{11} + \frac{T_{12}}{\rho_0 c} + \rho_0 c T_{21} + T_{22}\right|^2\right) \quad (6)$$

Equation (6) is incorporated in the Brüel & Kjær acoustic testing program to compute the *TL* values of test samples (Song and Bolton 2000; Olivieri *et al.* 2007).

Stiffness Law

A typical *TL* graph is composed of a stiffness-controlled region (S-region) in low frequency ranges and a mass law-controlled region (M-region) in high frequency ranges with increasing sound frequency (Irwin and Graf 1979). Hence, the stiffer a sound-absorbing sample is, the higher *TL* value it shows in the low frequency ranges. According to the definition (Ng and Hui 2008), the stiffness of materials can be expressed as,

$$S = \frac{1}{12} \times \left(\frac{Eh^3}{1-\nu^2}\right) \quad (7)$$

where *S*, *E*, *h*, and *v* are the bending stiffness, modulus of elasticity (MOE), sample thickness, and Poisson's ratio of the sample, respectively.

From Eq. 7, it can be seen that MOE and sample thickness significantly affect the stiffness of materials. The MOE and sample thickness can also lead to changes in the speed of longitudinal sound waves (C_p) in materials, and the subsequent sound resonance frequency (R_f). C_p and R_f are expressed as Eqs. (8) and (9), respectively (Wang *et al.* 2011),

$$C_p = \sqrt{\frac{E}{m(1-\nu^2)}} \quad (8)$$

$$R_{f\,ab} = 0.45 C_p h \left[\left(\frac{a}{\sqrt{\pi} r} \right)^2 + \left(\frac{b}{\sqrt{\pi} r} \right)^2 \right] \quad (9)$$

where m in Eq. 8 is the surface area density of the test sample and r, a, and b in Eq. 9 are the radius of the sample surface and integers (1, 2, …) from the order of sound wave resonance, respectively (Song and Bolton 2003). Berry and Nicolas (1994) represented the *TL* with a stiffness-controlled region using Eqs. 7 and 9 as,

$$TL_{stiffness} = 10 \log_{10} \left\{ \left(\frac{\pi f m}{\rho c} \right)^2 \left[1 - \left(\frac{R_f}{f} \right)^2 \right]^2 \right\} \quad (10)$$

where R_f represents sound resonance frequency ($f >> R_f$). It should be pointed out that the sample mounting has a significant impact of the severity of the impact of the resonance on the *TL* results (Satoh *et al.* 2014).

Mass Law

When incident sound waves hit a sample, the test sample vibrates due to the changes of ambient sound pressures. This vibration energy dissipates in and out of the sample during the sound transmission process, and the dissipation increases with the increase of the sample mass, *i.e.*, mass law (Lee *et al.* 2008). In the mass law, the *TL* value of a sound barrier sample is calculated as (Jones 1979),

$$TL_{Mass}(\theta, \omega) = 10 \log_{10} \left\{ 1 + \left(\frac{\omega m \cos\theta}{2\rho c} \right)^2 \right\} \quad (11)$$

where, ω, m, θ, and ρc are sound angular frequency, surface density of sample per unit area, angle of incident sound wave, and characteristic impedance of medium, respectively. A small-scale experiment using an impedance tube adopts normal sound waves where the angle of incident sound waves is perpendicular to test samples, *i.e.*, $\theta = 0$ and $\omega = 2\pi f$ with f as incident sound frequency (Folds and Loggins 1977; Lee and Xu 2009). The experimental setup for the impedance tube is based on plane wave theory, where the angle of incidence is perpendicular to the surface of the sample. The tube diameter and microphone spacing govern the useable frequency range of the setup to ensure that measurements are made within a valid frequency range.

EXPERIMENTAL

Materials

Composite sample preparation

Materials and formulations of each composite sample for acoustic testing are listed in Table 1.

Table 1. Materials and Formulations of Each Composite Sample Used for Acoustic Testing

Explanation	Formulation and Content	Supplier
Material	HDPE (HGB 0760)	ExxonMobil Co.
	Pine wood flour (100 mesh)	American Wood Fibers
	Precipitated calcium carbonate (PCC)	Domino Sugar Company
	Nanoclay (nanoMax®)	Nanocor Incorporation
PE Composite	1) PCC: 0, 20, 40% + HDPE	Lab blend
	2) Nanoclay: 0, 4, 8% + HDPE	Lab blend
WPC	1) PCC: 0, 20, 40% + wood: 10% + HDPE	Lab WPC blend
	2) Nanoclay: 0, 4, 8% + wood: 10%+ HDPE	Lab WPC blend

Wood flour (WF), precipitated calcium carbonate (PCC), and clay were dried at 85 °C for 24 h to remove most moisture in the materials prior to compounding. The PCC used in this experiment had an average size of 1.2 μm, and clay particles exhibited exfoliated forms as reported by the company. In the first step, a CW Brabender Intelli-torque twin-screw extrusion machine **(**CW Brabender Instruments, South Hackensack, NJ) was used to make HDPE and PCC or clay base blends (HDPE : PCC = 60 : 40; HDPE : clay = 92 : 8). In the second step, the pellets were further diluted with HDPE or blended with wood flour to meet the pre-determined mixing ratios and then extruded with a Leistritz Micro-27 co-rotating parallel twin-screw extruder (Leistritz Corp., Allendale, NJ). Materials and formulations for sample manufacturing are listed in Table 1. The blending temperature profiles were 155, 165, 175, 180, 180, 180, 180, 175, 170, 160, and 175 °C for PCC-filled composites and 155, 165, 170, 175, 175, 175, 175, 170, 160, 155, and 170 °C for clay-filled composites from feeding zone to die (11 heating sections), respectively. The extruder rotation speed was 60 rpm. The extruded blends were pelletized again and then dried in an oven at 85 °C for 24 h. The prepared pellets were compression molded by using a Wabash V200 hot press (Wabash, ID, USA). A 30-ton compression force was applied to the composite plates at 180 °C for 10 min; then the plates, which had a target thickness of 9 mm, were cooled to room temperature under the same pressure. The manufactured plates were water-jetted to produce acoustic samples with target diameters of 29 mm. The precisely machined samples allowed a good fit of test samples in the test tube without lateral pressure being applied to the sample edge.

Methods

Mechanical property measurement

Three-point flexural testing was performed using a model 5582 Instron testing machine (Instron Inc., Norwood, MA) at a crosshead speed of 3 mm/min. Each sample with a size of 125 mm (length) × 15 mm (width) × 9 mm (thickness) was prepared from the same composite plates as the acoustic samples.

A Tinius Olsen Mode 1892 impact tester (Tinius Olsen Inc., Horsham, PA) was used to test un-notched Izod impact strength according to the ASTM D256 (2007). Samples of size 63.5 mm (length) × 3 mm (width) × 9 mm (thickness) were prepared for the impact strength test. These samples were also acquired from the same composite panels as the acoustic samples by cross-cutting.

Acoustic property measurement

To measure the *TL* values of prepared acoustic samples, an impedance tube instrument from Brüel & Kjær (Nærum, Denmark) composed of power amplifier (Type 2706), transmission loss tube kit (Type 4206T), signal amplifier (Type 3560C-S29), and pulse FFT analysis program (Labshop ver. 16.01) was used, as shown in Fig. 1a.

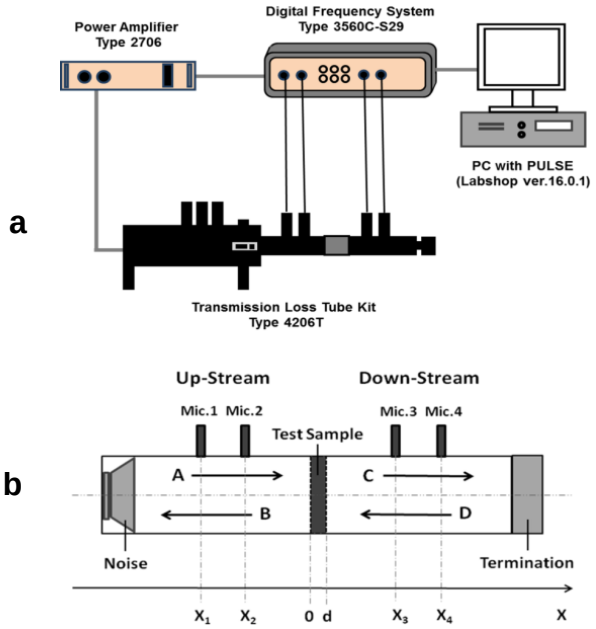

Fig. 1. Schematic diagram of (a) hardware setup and (b) the *TL* measurement in an impedance tube

A small tube (500 to 6400 Hz) set-up was chosen for the analysis. Prior to acoustic testing, petroleum jelly (*i.e.*, Vaseline®) was added to sample edges such that they fit into the test tube without much lateral force from the tube wall and so sound leakages would be minimized. Sample dimensions and weights were measured and then used to calculate the surface area density of each sample. To get a better *TL* curve without noise fluctuations, respective FFT curves were smoothed by 1/3 octave band width using the computer software from Brüel & Kjær.

RESULTS AND DISCUSSION

Basic Properties of Mineral-filled HDPE and WPCs

The densities of clay, PCC, and HDPE were 1.60, 2.60, and 0.96 g/cm^3, respectively (Klyosov 2007; Wypych 2010; Kim *et al.* 2012). Thus, the addition of clay and PCC in the HDPE matrix increased the surface area density of the filled HDPE (Table 2). Pure HDPE had a surface area density of 8.59 kg/m^2. The surface area density increased to 8.95 kg/m^2 at 8% clay loading level and to 10.83 kg/m^2 at 40% PCC level. The WPCs with 10% WF filled with clay or PCC had similar surface area densities compared with corresponding clay or PCC filled HDPE, respectively. Thus, the use of 10% WF did not significantly alter the composite area density.

Table 2. Mechanical Properties (MOE, MOR, and Impact Strength), Stiffness, and Area Density of Mineral-filled HDPE Composites and WPCs as a Function of Filler Content

System	Filler (%)	MOE[a] (GPa)	MOR[a] (MPa)	Impact Strength[a] (kJ/m^2)	Stiffness of Unit Area (×10^5 N/m^2)	Area Density of Unit Area (kg/m^2)
Clay Only	0	1.20 (0.02)	41.57 (1.21)	No Break	119.05	8.59
	4	1.31 (0.01)	33.17 (0.05)	5.90 (0.11)	129.47	8.79
	8	1.34 (0.05)	30.42 (0.98)	5.18 (0.19)	131.94	8.95
PCC Only	20	1.47 (0.05)	46.20 (0.56)	11.03 (2.35)	144.47	9.75
	40	1.51 (0.04)	32.49 (0.47)	7.00 (0.65)	148.41	10.83
Clay + WF	0 + 10	1.39 (0.03)	37.47 (0.82)	17.98 (0.89)	136.61	8.26
	4 + 10	1.45 (0.06)	37.67 (1.04)	10.19 (2.21)	141.99	8.47
	8 + 10	1.47 (0.06)	33.22 (0.39)	6.58 (1.50)	143.43	8.68
PCC + WF	20 + 10	1.64 (0.05)	37.14 (1.50)	13.50 (2.74)	159.73	9.57
	40 + 10	1.49 (0.04)	34.33 (0.17)	4.37 (0.36)	145.12	10.66

[a] Numbers in parenthesis are standard deviations based on five samples. MOE – Modulus of Elasticity, MOR- Modulus of Rupture.

The neat HDPE sample had an MOE value of 1.2 GPa. At 4% and 8% clay loading levels, the modulus increased to 1.31 GPa and 1.34 GPa, respectively. Early work in this field (Wu *et al.* 2007) attributed the modulus increase to exfoliation of clay nanoplatelets in the plastic matrix. The degree of exfoliation depends on mixing and the use of coupling agents. The PCC filled HDPE also showed a higher modulus than neat-HDPE, probably due to higher filler content (Kim *et al.* 2012). The corresponding stiffness for both types of composites also increased with increased clay or PCC content. On the other hand, bending MOR and impact strength decreased with increased clay or PCC content. Possible particle aggregation in the HDPE matrix, which creates stress concentration at the particle-matrix interface, led to decreased overall composite strength.

For clay-filled WPCs with 10% WF, increased clay loadings led to some improvements in MOE values (*e.g.*, 1.39 GPa at 0% clay level and 1.47 GPa at 8% clay level). This indicates that there was an overall modulus enhancement in clay-filled WPCs compared with corresponding clay-filled HDPE, showing synergetic effects of clay platelets and wood fibers. For PCC-filled WPCs with 10% WF, MOE values were obviously increased at the 20% PCC level, but somewhat reduced at the 40% PCC level in comparison with corresponding PCC-filled HDPE. In impact strength testing, decreased trends were shown with increased clay or PCC content. The reduced strength properties of filled composites are attributed to the aggregation of filler particles in the HDPE matrix (Kim *et al.* 2012).

General *TL* Curves of Filled HDPE and WPCs

Figure 2 shows measured *TL* curves for clay- (Fig. 2a) and PCC- (Fig. 2b) filled HDPE and WPC materials. The *TL* curves shifted upwards as clay or PCC level increased, indicating improved *TL* properties at higher filler loading levels. The surface area density of clay-filled HDPE was only slightly higher than that of neat HDPE (Table 2). Hence, the observed *TL* improvements, especially in a low frequency range, probably indicate the effect of nano-clay in filled HDPE.

The clay particles after intercalation and exfoliation had platelet shapes with thicknesses in the nanometer range and were distributed in the plastic matrix (Gopakumar *et al.* 2002; Ton-That *et al.* 2004; Ataeefard and Moradian 2011).

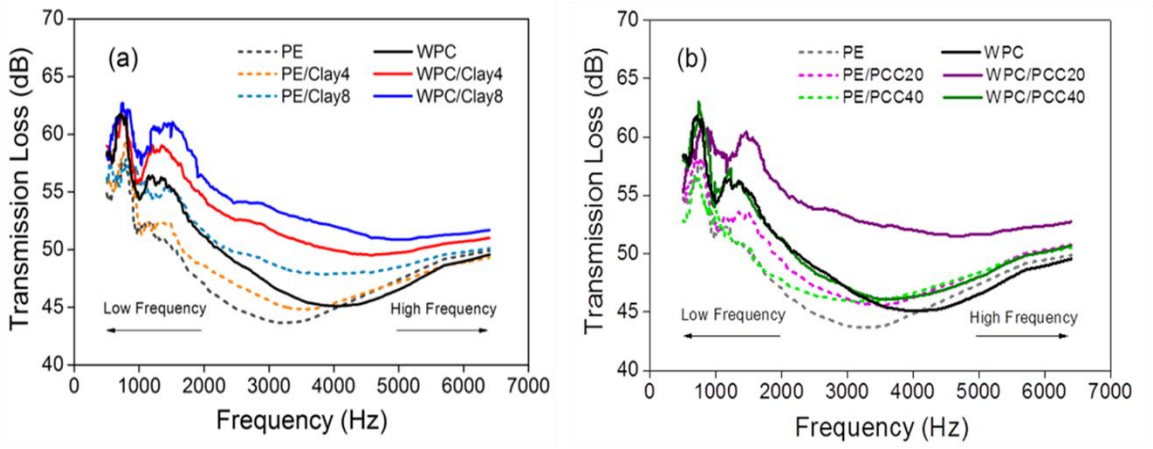

Fig. 2. Comparisons of *TL* curves between (a) clay-filled HDPE and WPCs and (b) PCC-filled HDPE and WPCs

The platelets can help deflect sound waves and increase their energy dissipation pathway as heat, leading to increased *TL* values (Bharadwaj 2001; Picard *et al.* 2007; Lee *et al.* 2008). The addition of PCC in HDPE led to a distinctively increased surface area density. The increased surface area density helped improve *TL* values of PCC-filled HDPE in comparison with neat HDPE. However, the 40% PCC-filled HDPE showed both a lower *TL* curve in the low frequency range and a higher *TL* curve in the high frequency range, which was different from the 20% PCC-filled HDPE, as shown in Fig. 2b.

The incorporation of 10% WF in the clay- or PCC-filled HDPE led to overall *TL* improvements in comparison with corresponding clay- or PCC-only-filled HDPE. The above results show a synergistic effect of clay or PCC and wood particles in the composites through blocking/reflecting the incident sound waves and enhancing composite stiffness. The relatively large *TL* differences in the low-frequency range indicate stiffness controls and the relatively small *TL* differences in the high-frequency range indicate mass controls in the *TL* property of the filled composites, respectively.

Comparison of *TL* with Mass and Stiffness Law Predictions

Typical experimental *TL* curves of clay- or PCC-filled HDPE and WPCs are shown in Figs. 3 and 4, respectively, in comparison with their corresponding mass law and stiffness law *TL* prediction lines. The mass law *TL* equation used here is a modified form of Eq. 6 (Lee and Xu 2009):

$$TL_{normal} = 20\log_{10}(fm) - 42.5 \quad (12)$$

The stiffness law *TL* equation was adapted from Eq. 10, and the first (a = 1, and b = 1) and second (a = 1 and b = 2) orders of sound resonance frequencies were used to get two stiffness *TL* prediction lines (*i.e.*, stiffness-1 and stiffness-2).

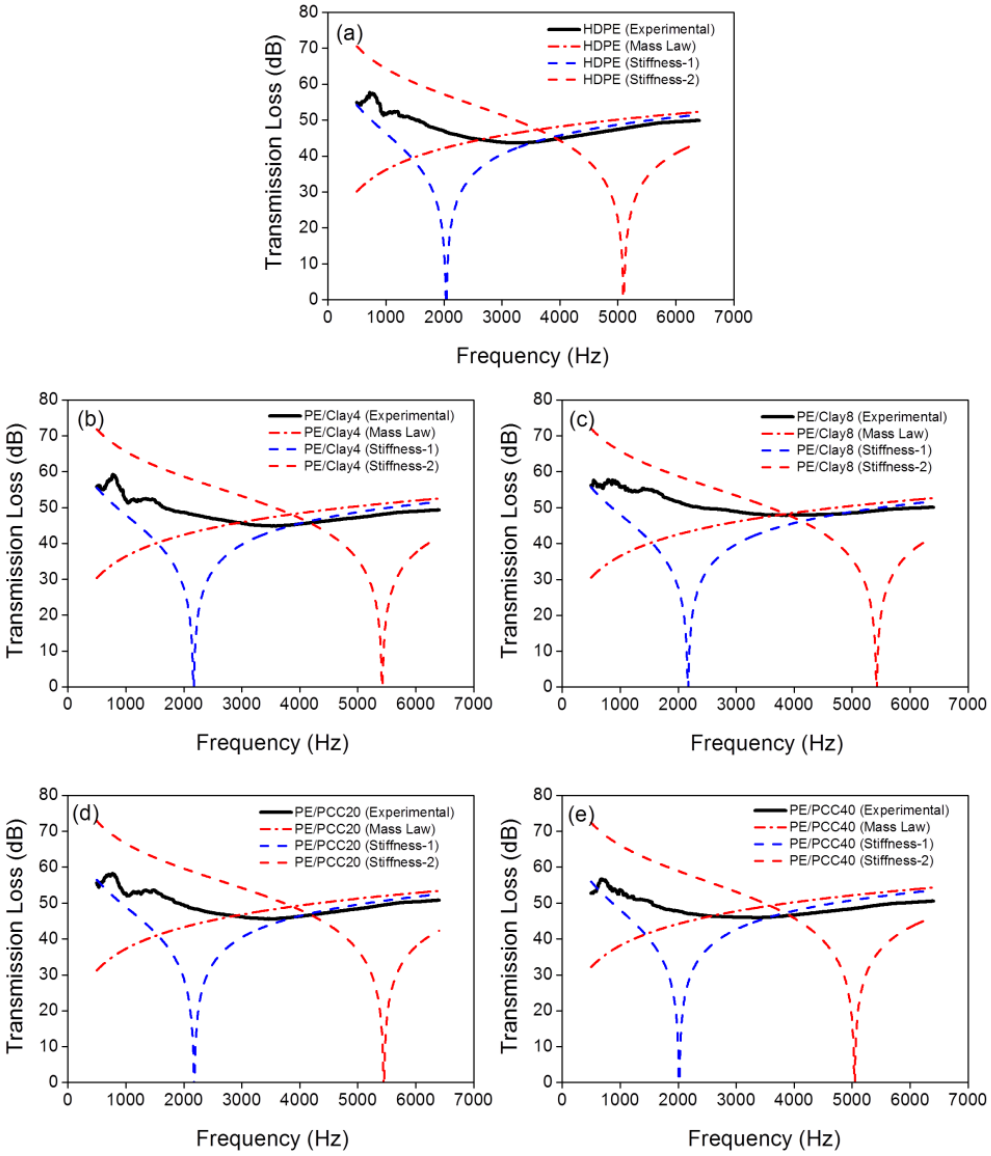

Fig. 3. Comparisons of experimental *TL* curves of filled HDPE in comparison with mass and stiffness law *TL* predictions. (a) HDPE, (b) HDPE/Clay4, (c) HDPE/Clay8, (d) HDPE/PCC20, and (e) HDPE/PCC40

Experimental *TL* curves decreased as sound frequency increased and then increased after passing a certain frequency level (designated as experimental resonance frequency – R_{FE}). Predicted stiffness-1 and stiffness-2 *TL* curves showed two resonance frequencies (R_{FS1} and R_{FS2}, respectively) and mass law *TL* curves formed linear lines after an initial rapid *TL* increase at the low frequency range.

The effect of filler loading and filler type on the shape of the filled *TL* curves seems to be small. A comparison among the experimental and predicted stiffness and mass law *TL* curves indicates a well-defined stiffness-controlled region (S-region: left) and mass controlled region (M-region: right).

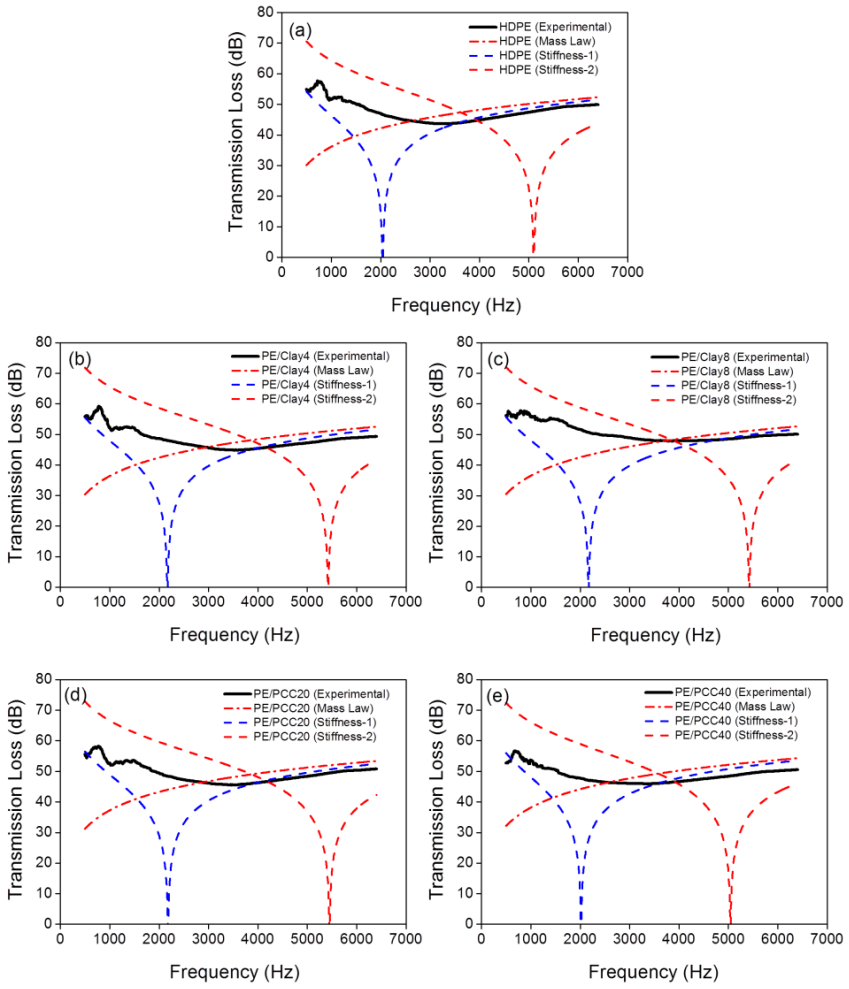

Fig. 4. Comparisons of experimental *TL* curves of filled WPCs in comparison with mass and stiffness law *TL* predictions. (a) WPC, (b) WPC/Clay4, (c) WPC/Clay8, (d) WPC/PCC20, and (e) WPC/PCC40

The experimental *TL* curves of filled HDPE and WPCs (Fig. 3a and 4a) show similar trends to their corresponding mass law *TL* predictions for the M-region. This result is similar to the previous experimental *TL* data using mica-filled PVC with a thickness of 1 mm (Wang *et al.* 2011). However, for the S-region, there are some differences between the results from the two studies.

While the published experimental *TL* curves had similar features to their corresponding stiffness-1 *TL* predictions, the experimental *TL* curves from the current work are positioned in between the stiffness-1 and stiffness-2 *TL* predictions. The different experimental *TL* features between the two studies for the S-region may be related with stiffness differences.

When the stiffness equation described in Eq. 8 is considered, the stiffness value is significantly affected by the thickness of test samples (*i.e.*, 729 times difference between 1 mm and 9 mm) and increased sample thickness led to remarkable stiffness value differences. Thus, the increased stiffness values from the test samples with 9-mm thicknesses resulted in the remarkable *TL* improvements in the S-region.

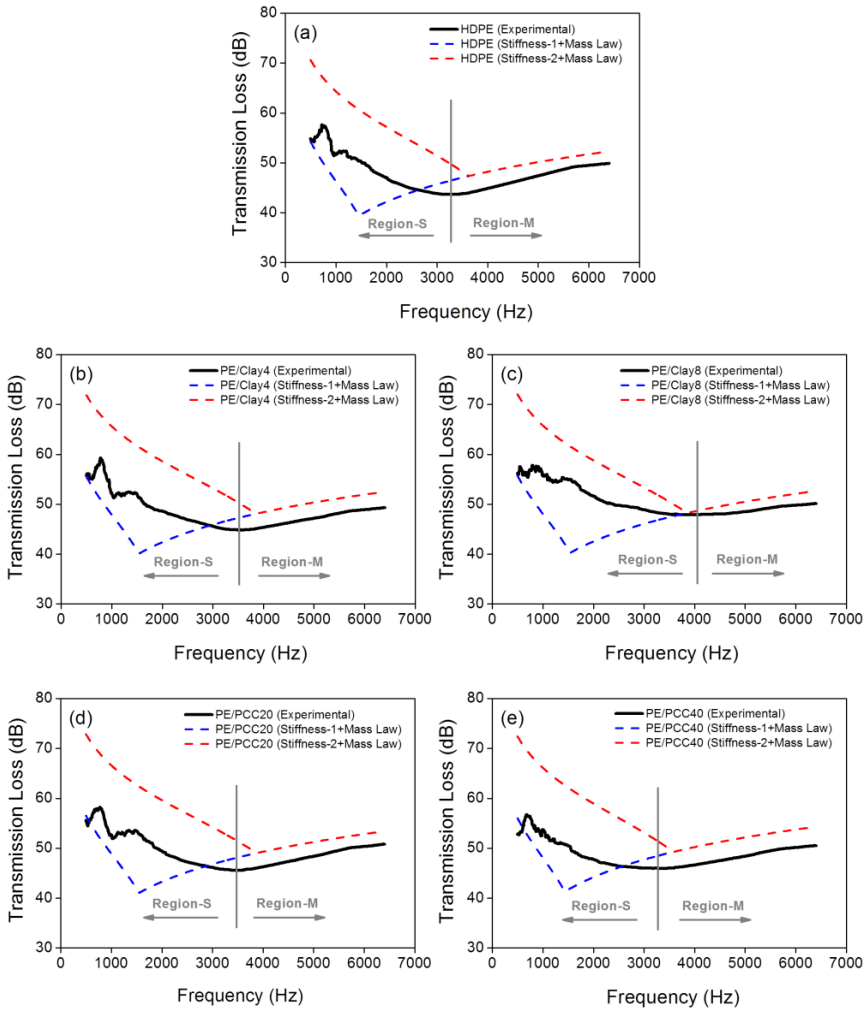

Fig. 5. Comparisons of experimental *TL* curves of filled HDPE in comparison with combined *TL* predictions. (a) HDPE, (b) HDPE/Clay4, (c) HDPE/Clay8, (d) HDPE/PCC20, and (e) HDPE/PCC40

The stiffness-1 and stiffness-2 *TL* curves form two intersection points ($R_{S1\text{-}M\text{-}IP}$ and $R_{S2\text{-}M\text{-}IP}$, respectively) with the mass law *TL* curve as shown in Fig. 5 (filled HDPE) and Fig. 6 (filled WPCs).

The experimental *TL* curves of filled HDPE and WPCs are better approximated by the combined *TL* predictions from their corresponding stiffness-1 and stiffness-2 *TL* curves for the S-region and from mass law *TL* curves for the M-region. Table 3 shows a comparison of the R_{FE}, R_{FS1}, R_{FS2}, $R_{S1\text{-}M\text{-}IP}$, and $R_{S2\text{-}M\text{-}IP}$ values for various composites. While the R_{FE} values of filled HDPE composites are located between the corresponding $R_{S1\text{-}M\text{-}IP}$ and $R_{S2\text{-}M\text{-}IP}$ values, those of filled WPCs are closer to the corresponding $R_{S2\text{-}M\text{-}IP}$ values or are located to the right side of them. From the above result, it can be noticed that the MOE and stiffness increases of the test samples led to the experimental *TL* improvements in the S-region and these consequently shifted their R_{FE} values to the higher frequency range.

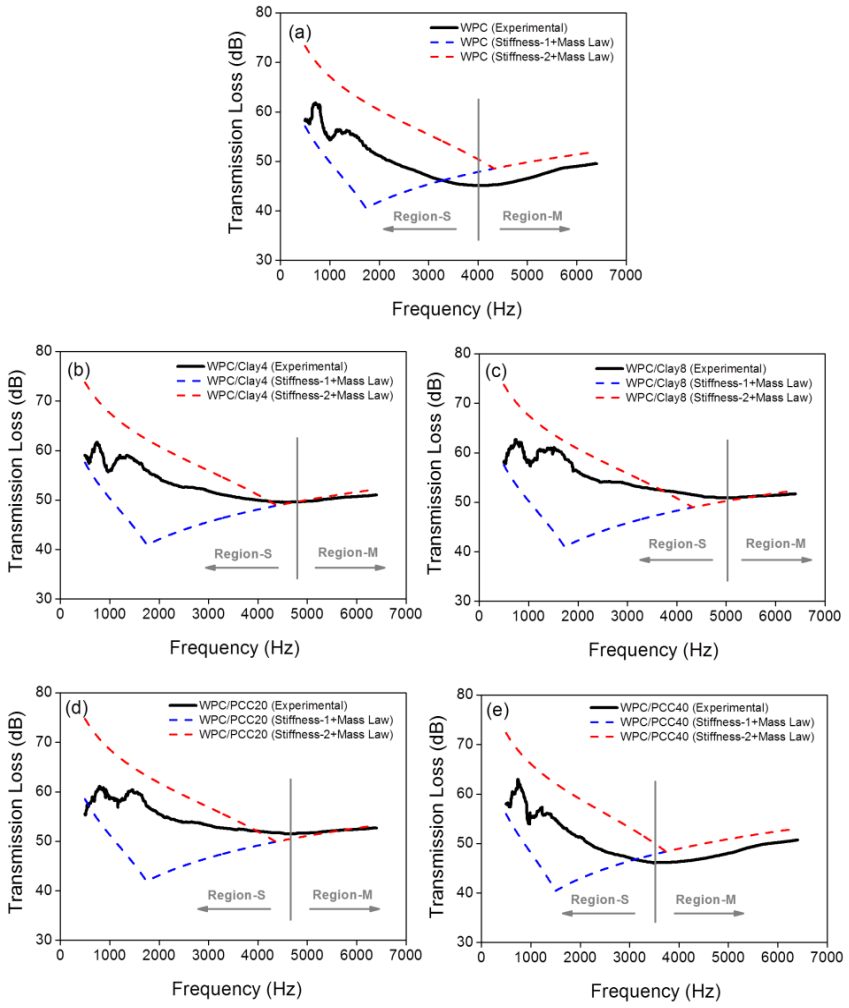

Fig. 6. Comparisons of experimental *TL* curves of filled WPCs in comparison with combined *TL* Predictions. (a) WPC, (b) WPC/Clay4, (c) WPC/Clay8, (d) WPC/PCC20, and (e) WPC/PCC40

Table 3. Summary of Sound Transmission Property of Filled HDPE and WPCs

Sample Name	Experimental Resonance Frequency R_{FE} (Hz)	Predicted Resonance Frequency		Stiffness-Mass Law Curves Intersection Points	
		R_{FS1} (Hz)	R_{FS2} (Hz)	$R_{S1\text{-}M\text{-}IP}$ (Hz)	$R_{S2\text{-}M\text{-}IP}$ (Hz)
HDPE	3216	2040	5099	1448	3624
HDPE/Clay4	3592	2168	5421	1540	3852
HDPE/Clay8	3792	2169	5422	1540	3852
HDPE/PCC20	3564	2179	5448	1548	3872
HDPE/PCC40	3416	2016	5041	1432	3580
WPC	4080	2435	6087	1728	4324
WPC/Clay4	4572	2467	6169	1752	4380
WPC/Clay8	4980	2432	6079	1728	4320
WPC/PCC20	4588	2455	6138	1744	4360
WPC/PCC40	3524	2002	5006	1424	3556

Effect of Filler Type and Loading Level on Mean *TL*

Averaged *TL* (*A-TL*) values of clay or PCC filled HDPE and WPCs were plotted for S-region and M-region as a function of filler content, as shown in Fig. 7. Clay-filled HDPE and WPCs showed improved *A-TL* values for both S-region and M-region with the increase of clay content (Fig. 7a). While the clay-filled HDPE had more obviously improved *A-TL* values at only 8% clay level, the clay-filled WPCs showed enhanced *A-TL* values even at 4% clay level, indicating the synergistic effect of WF. PCC filled HDPE and WPCs had their highest *A-TL* values at 20% PCC level. At this level, *A-TL* values were much improved with the use of 10% WF for S-region. However, further increase of PCC content (*e.g.*, 40% PCC level) resulted in stiffness decreases, leading to decreased *A-TL* values.

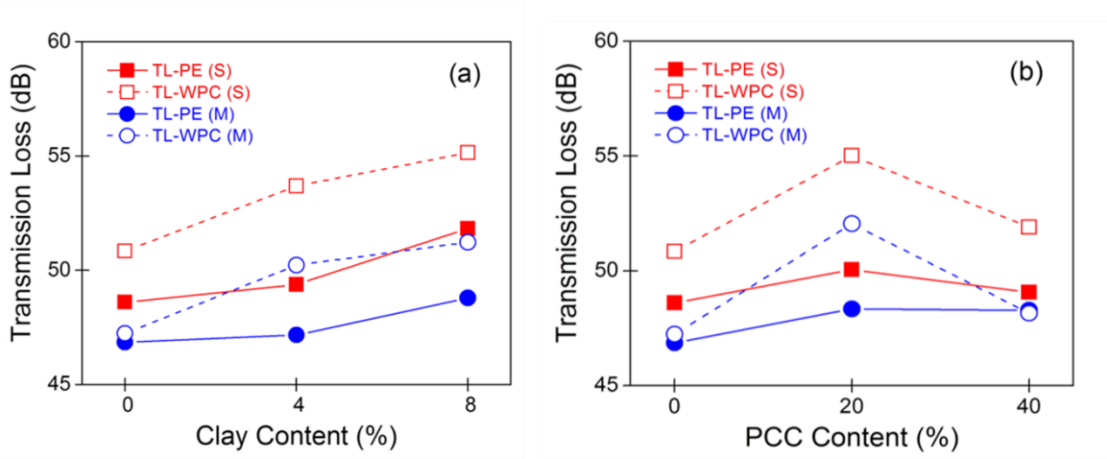

Fig. 7. Comparisons of experimental *TL* curves of filled WPCs in comparison with combined *TL* predictions; (a) WPC, (b) WPC/Clay4, (c) WPC/Clay8, (d) WPC/PCC20, and (e) WPC/PCC40

CONCLUSIONS

1. The experimental sound transmission loss (*TL*) curves of filled high-density polyethylene (HDPE) and wood plastic composites (WPCs) were better approximated with the combined *TL* predictions from their corresponding stiffness-1 and stiffness-2 *TL* for stiffness-controlled region and mass law *TL* for mass law-controlled region. Analyses of the combined *TL* predictions and *A-TL* values in clay-filled WPCs suggested the synergistic effect of clay and WF in the composites.
2. The stiffness law, mass law, and their combined predictions were used to further analyze the *TL* data of the materials. Experimental *TL* results showed that the addition of clay or PCC and/or WF fillers led to general resonance frequency and *TL* increases of filled composites. However, at high filler loading level (*e.g.*, 40% PCC filled WPC), decreased composite stiffness from filler aggregations led to reduced *TL* values.
3. The *TL* analysis showed that stiffness and surface area density were major factors influencing the sound insulation property of the filled composites.

4. As filler loading level was increased, the modulus and stiffness of filled composites increased accordingly. However, the surface area density of filled composites varied depending on the density of fillers.

ACKNOWLEDGMENTS

This collaborative study was carried out with support from a LSU project funded by Korea Forest Research Institute, 'Forest Science & Technology Projects (No. S211314L010140)' provided by the Korea Forest Service, Natural Science Foundation of China (No.31300482), and the Natural Science Foundation of Jiangsu Province (No. BK20130966).

REFERENCES CITED

ASTM D256 (2007). "Standard test method for determining the izod pendulum impact resistance of plastics," ASTM International, West Conshohocken, PA.

ASTM E2611 (2009), "Standard test method for measurement of normal incidence sound transmission of acoustical materials based on the transfer matrix method," ASTM International, West Conshohocken, PA.

Ataeefard, M., and Moradian, S. (2011). "Polypropylene/organoclay nanocomposites: Effects of clay content on properties," *Polymer-Plastics Technology and Engineering* 50(7), 732-739. DOI: 10.1080/03602559.2010.551438

Berry, A., and Nicolas, J. (1994). "Structural acoustics and vibration behavior of complex panels," *Applied Acoustics* 43(3), 185-215. DOI: 10.1016/0003-682X(94)90047-7

Bharadwaj, R. K. (2001). "Modeling the barrier properties of polymer-layered silicate nanocomposites," *Macromolecules* 34(26), 9189-9192. DOI: 10.1021/ma010780b

Cotana, F., Rossi, F., Nicolini, A., and Simoni, S. (2007). "Acoustic tests on original concrete and inert mixture materials," 14th International Congress on Sound & Vibration, July 9-12, Cairns, Australia.

Folds, D. L., and Loggins, C. D. (1977). "Transmission and reflection of ultrasonic-waves in layered media," *Journal of the Acoustical Society of America* 62(5), 1102-1109. DOI: 10.1121/1.381643

Gopakumar, T. G., Lee, J. A., Kontopoulou, M., and Parent, J. S. (2002). "Influence of clay exfoliation on the physical properties of montmorillonite/polyethylene composites," *Polymer* 43(20), 5483-5491. DOI: 10.1016/S0032-3861(02)00403-2

Irwin, J. D., and Graf, E. R. (1979). *Industrial Noise and Vibration Control*, Prentice-Hall, Englewood Cliffs, NJ.

Jayaraman, K. A. (2005). *Acoustical Absorptive Properties of Nowovens*, M.S. thesis, North Carolina State University, Raleigh, NC.

Jones, R. E. (1979). "Intercomparisons of laboratory determinations of airborne sound-transmission loss," *Journal of the Acoustical Society of America* 66(1), 148-164. DOI: 10.1121/1.383068

Kim, B. J., Yao, F., Han, G. P., and Wu, Q. L. (2012). "Performance of bamboo plastic composites with hybrid bamboo and precipitated calcium carbonate fillers," *Polymer Composites* 33(1), 68-78. DOI: 10.1002/pc.21244

Klyosov, A. A. (2007). *Wood-Plastic Composites*, John Wiley & Sons, Hoboken, NJ.

Kotzen, B., and English, C. (1999). *Environmental Noise Barriers: A Guide to Their Acoustic and Visual Design*, Routledge, New York.

Lee, C. M., and Xu, Y. (2009). "A modified transfer matrix method for prediction of transmission loss of multilayer acoustic materials," *Journal of Sound and Vibration* 326(1-2), 290-301. DOI: 10.1016/j.jsv.2009.04.037

Lee, J. C., Hong, Y. S., Nan, R. G., Jang, M. K., Lee, C. S., Ahn, S. H., and Kang, Y. J. (2008). "Soundproofing effect of nano particle reinforced polymer composites," *Journal of Mechanical Science and Technology* 22(8), 1468-1474. DOI: 10.1007/s12206-008-0419-4

Lee, J. W., Lee, J. C., Pandey, J., Ahn, S. H., and Kang, Y. J. (2010). "Mechanical properties and sound insulation effect of ABS/carbon-black composites," *Journal of Composite Materials* 44(14), 1701-1716. DOI: 10.1177/0021998309357673

Ng, C. F., and Hui, C. K. (2008). "Low frequency sound insulation using stiffness control with honeycomb panels," *Applied Acoustics* 69(4), 293-301. DOI: 10.1016/j.apacoust.2006.12.001

Olivieri, O., Bolton, J. S., and Yoo, T. W. (2006). "Measurement of transmission loss of materials using a standing wave tube," *Proceedings of Inter-Noise*, Honolulu, Hawaii, pp 3515-3522.

Olivieri, O., Bolton, J. S., and Yoo, T. W. (2007). *Measurement of Normal Incidence Transmission Loss and Other Acoustical Properties of Materials Placed in a Standing Wave Tube*, Brüel & Kjær Technical Review, No. 1, 1-44.

Picard, E., Vermogen, A., Gerard, J. F., and Espuche, E. (2007). "Barrier properties of nylon 6-montmorillonite nanocomposite membranes prepared by melt blending: Influence of the clay content and dispersion state - Consequences on modelling," *Journal of Membrane Science* 292(1-2), 133-144. DOI: 10.1016/j.memsci.2007.01.030

Raveendra, S., Zhang, W., Challa, D., and Hong, K. (2005). "Improving the acoustical performance of poroelastic materials," *SAE Technical Paper* 2005-01-2283, 2005, DOI:10.4271/2005-01-2283.

Satoh, T., Kimura, M., Yamaguchi, M., and Kunio, J. (2014). "An impedance tube measurement technique for controlling elastic behavior of test samples," The 43rd International Congress on Noise Control Engineering, Melbourne, Australia.

Song, B. H., and Bolton, J. S. (2000). "A transfer-matrix approach for estimating the characteristic impedance and wave numbers of limp and rigid porous materials," *Journal of the Acoustical Society of America* 107(3), 1131-1152. DOI: 10.1121/1.428404

Song, B. J., and Bolton, J. S. (2003). "Investigation of the vibrational modes of edge-constrained fibrous samples placed in a standing wave tube," *Journal of the Acoustical Society of America* 113(4), 1833-1849. DOI: 10.1121/1.1548155

Ton-That, M. T., Perrin-Sarazin, F., Cole, K. C., Bureau, M. N., and Denault, J. (2004). "Polyolefin nanocomposites: Formulation and development," *Polymer Engineering and Science* 44(7), 1212-1219. DOI: 10.1002/pen.20116

Wang, X., You, F., Zhang, F. S., Li, J., and Guo, S. Y. (2011). "Experimental and theoretic studies on sound transmission loss of laminated mica-filled poly(vinyl chloride) composites," *Journal of Applied Polymer Science* 122(2), 1427-1433. DOI: 10.1002/app.34047

Wu, Q., Lei, Y., Clemons, C. M., Yao, F., and Xu, Y. (2007). "Influence of nanoclay on properties of HDPE/wood composites," *Journal of Applied Polymer Science* 106(6), 3958-3966. DOI: 10.1002/app.27048

Wypych, G. (2010). *Handbook of Fillers*, ChemTec Publishing, Ontario, Canada.

Yilmaz, N. D. (2009). *Acoustic Properties of Biodegradable Nonwovens*, Ph.D. dissertation, North Carolina State University, Raleigh, NC.

Yoo, T., Bolton, J. S., and Alexander, J. H. (2005). "Prediction of random incidence transmission loss based on normal incidence four-microphone measurements," The 2005 Congress and Exposition on Noise Control Engineering, Rio de Janeiro, Brazil. 10 pp.

Yousefzadeh, M., Mahjoob, M., Mohammadi, N., and Shahsavari, A. (2008). "An experimental study of sound transmission loss (STL) measurement techniques using an impedance tube," Annual Meeting of the Acoustical Society of America, June 30-July 4, Paris, France, pp. 965-968.

Article submitted: June 10, 2014; Peer review completed: August 17, 2014; Revised version received: November 12, 2014; Accepted: November 13, 2014; Published: November 25, 2014.